2018 IEEE-RAS 18th International Conference on Humanoid Robots (Humanoids)
Beijing, China, November 6-9, 2018

A Self-Adaptive Robot Control Framework for Improved Tracking and Interaction Performances in Low-Stiffness Teleoperation

Adriano Scibilia[1,2], Marco Laghi[1,3], Elena De Momi[2], Luka Peternel[1], and Arash Ajoudani[1]

Abstract— **The improved adaptability of a robotic teleoperation system to unexpected disturbances in remote environments can be achieved by compliance control. Nevertheless, complying with all types of interaction forces while performing realistic manipulation tasks may deteriorate the teleoperation performance. For instance, the loading effect of the objects and tools that are held and manipulated by the robot can introduce undesired deviations from the reference trajectories in case of low-stiffness (or high payload) teleoperation. Although this can be addressed by updating the robot dynamics with the external loading effect, a sudden loss of the object may also generate undesired and potentially dangerous robot behaviours. To address this problem, we propose a novel and self-adaptive teleoperation framework. The method uses the feedback from robot's force sensors to recognize the interaction aspects that must be compensated by robot dynamics. Thanks to this online compensation, the slave robot reduces the tracking error with respect to the commanded motion by the human operator, while performing complex interactive tasks without the haptic feedback. The robot local controller also includes an energy tank based passivity paradigm to be able to manage unexpected collisions or a contact loss without resulting in an unsafe behaviour. We validate the proposed approach by experiments on a torque-controlled robotic arm performing manipulation tasks that require both object manipulation and environment interaction.**

I. Introduction

The role of robotics in modern industry has been increasing for decades, from mining to automotive sector, where robots are performing tasks that humans either do not want or cannot do. In the past, robots were generally large, heavy and stiff, therefore they were physically separated, often by a cage, from their human operators for safety reasons. They had to operate with a complete knowledge of the environment and a detailed planning of the task.

Recently developed technologies have enabled robots to move from the predictable industrial environments to more unpredictable ones. The applications range from health-care and domestic assistance to disaster response scenarios, where the robots are helping people and constantly interacting with unknown and dynamically changing environments. In this direction, the integration of robots in teleoperation scenarios has gained the confidence to take on real-world challenges, with the advantage of combining robotics strength and precision, with humans' superior cognitive capabilities and understanding of the tasks.

[1]Human-Robot Interfaces and physical Interaction Lab and SoftBots Lab, Advanced Robotics, Istituto Italiano di Tecnologia, Genova, Italy.
[2] NearLab, Politecnico di Milano, Milano, Italy.
[3] Centro di Ricerca "E.Piaggio", Universit di Pisa, Pisa, Italy.
`{adriano.scibilia, marco.laghi, luka.peternel, arash.ajoudani}@iit.it`

An important aspect to be considered is that, the teleoperated robot's precision in tacking the human commands should be adjustable when interacting with unknown or unpredictable environments to ensure a safe and effective task execution [1]. To this end, impedance control provides a solution to adjust the dynamic response of the robot to external interaction forces by establishing a suitable virtual mass-spring-damper system at the end-effector [2]. Through this control framework, the excessive contact forces between the manipulator and the environment can be prevented by modulating the stiffness of the teleoperated robot at the end-effector [3]–[5]. This behaviour is crucial when performing remote manipulation in unknown and cluttered environments [6], to comply with the external disturbances, or when humans are constantly present in the robot workspace, which requires the robot to operate in a low impedance range to ensure a safe interaction with the human [7].

On the other hand, complying with all types of interaction forces may deteriorate the teleoperation performance. For instance, additional loads will introduce undesired deviations of the robot end-effector from the operator's reference position commands. To avoid this effect, the loading effect of the object should be included into the robot's gravity compensation scheme (e.g., see [8]–[10]). However, in an unpredictable and dynamically varying environment, the external disturbances may result in lost contact and cause potential instabilities due to the load-compensatory robot dynamics.

To address this problem, this paper presents a novel control framework to enable robot adaptation to external payloads while avoiding potential instabilities when the contact is suddenly lost. The proposed teleoperation framework enables the operator to control robot movements in space, whose endpoint stiffness is set to low values with the purpose of maintaining a safe and adaptive behavior when unexpected contacts occur. The local robot impedance controller is enriched with a payload adaptation scheme when an object is detected at the robot's end-effector. To ensure the stability of the proposed control action, we implement a passivity controller based on the Energy-Tank paradigm [11]–[13]. The energy tank regulates the action of the robot controller when an unexpected contact loss occurs during the task execution. The main feature of the proposed energy tank is that it is able to distinguish force changes introduced by the object and the ones arising from external interactions that does not require any change in the control action.

To validate the proposed method we perform experiments on a teleoperated KUKA Light Weight Robot, equipped with the Pisa/IIT SoftHand [14]. The task of the human operator is to teleoperate a very compliant robot arm to grasp and pick up a heavy object and move it to a predefined position. The contact loss occurs unexpectedly during the task and the controller's ability to cancel out the unstabilizing payload effect is evaluated. This scenario is tasted with and without the proposed control method.

II. Methods

A. Impedance control

Rigid body dynamics of a robot with *n* degrees of freedom can be formally described by the Euler-Lagrange model

$$\mathbf{M}(\mathbf{q})\ddot{\mathbf{q}} + \mathbf{C}(\mathbf{q},\dot{\mathbf{q}})\dot{\mathbf{q}} + \mathbf{G}(\mathbf{q}) = \boldsymbol{\tau}_c + \boldsymbol{\tau}_{ext}, \tag{1}$$

where $\mathbf{q}, \dot{\mathbf{q}}, \ddot{\mathbf{q}} \in \mathbb{R}^n$ are the joint position, velocity and acceleration vectors, respectively, $\mathbf{M}(\mathbf{q}) \in \mathbb{R}^{n\times n}$ is the mass matrix, $\mathbf{C}(\mathbf{q},\dot{\mathbf{q}})\dot{\mathbf{q}} \in \mathbb{R}^n$ is the Coriolis and centrifugal vector, and $\mathbf{G}(\mathbf{q}) \in \mathbb{R}^n$ is the gravity term. The input of the system is represented by the controlled torque vector $\boldsymbol{\tau}_c \in \mathbb{R}^n$, while vector $\boldsymbol{\tau}_{ext} \in \mathbb{R}^n$ comprises all externally applied torques. The position of the end-effector in the Cartesian space can be described by a set of local coordinates $\mathbf{x} \in \mathbb{R}^m$. If the forward kinematics $\mathbf{x} = f(\mathbf{q})$ is known, velocity $\dot{\mathbf{x}}$ and acceleration $\ddot{\mathbf{x}}$ in Cartesian space can be computed via the Jacobian $\mathbf{J}(\mathbf{q}) = \frac{\partial f(\mathbf{q})}{\partial \mathbf{q}}$

$$\dot{\mathbf{x}} = \mathbf{J}(\mathbf{q})\dot{\mathbf{q}}, \tag{2}$$

$$\ddot{\mathbf{x}} = \mathbf{J}(\mathbf{q})\ddot{\mathbf{q}} + \dot{\mathbf{J}}(\mathbf{q})\dot{\mathbf{q}}. \tag{3}$$

The external wrenches $\mathbf{F}_{ext}$ applied to the end-effector can also be mapped to the joint space through the Jacobian matrix of the manipulator $\mathbf{J}(\mathbf{q}) \in \mathbb{R}^{m\times n}$, so that $\boldsymbol{\tau}_{ext} = \mathbf{J}(\mathbf{q})^T\mathbf{F}_{ext}$.

The objective of the impedance controller is to provide a dynamical relationship between motion and external force as

$$\boldsymbol{\Omega}_d\ddot{\tilde{\mathbf{x}}} + \mathbf{D}_d\dot{\tilde{\mathbf{x}}} + \mathbf{K}_d\tilde{\mathbf{x}} = \mathbf{F}_{ext}, \tag{4}$$

where $\tilde{\mathbf{x}}(t) = \mathbf{x}(t) - \mathbf{x}_d(t)$ represents the difference between the actual and the desired ($\mathbf{x}_d(t) \in \mathbb{R}^m$) end-effector position, while $\boldsymbol{\Omega}_d \in \mathbb{R}^{m\times m}$, $\mathbf{K}_d \in \mathbb{R}^{m\times m}$ and $\mathbf{D}_d \in \mathbb{R}^{m\times m}$ are the desired inertia, stiffness and damping matrices, respectively. The inertia matrix and the Coriolis/centrifugal matrix can be represented with respect to the Cartesian space coordinates as

$$\boldsymbol{\Omega}(\mathbf{x}) = (\mathbf{J}(\mathbf{q})\mathbf{M}(\mathbf{q})^{-\mathbf{1}}\mathbf{J}(\mathbf{q})^T)^{-1} \tag{5a}$$

$$\boldsymbol{\mu}(\mathbf{x},\dot{\mathbf{x}}) = \mathbf{J}(\mathbf{q})^{-T}[\mathbf{C}(\mathbf{q},\dot{\mathbf{q}}) - \mathbf{M}(\mathbf{q})\mathbf{J}(\mathbf{q})^{-\mathbf{1}}\dot{\mathbf{J}}(\mathbf{q})]\mathbf{J}(\mathbf{q})^{-1} \tag{5b}$$

Note that a pseudo-inverse of Jacobian should be used instead of inverse when the robot has redundant degrees of freedom. As demonstrated in [15], it is possible to set $\boldsymbol{\Omega}_d = \boldsymbol{\Omega}(\mathbf{x})$ to avoid the need for a direct feedback of $\mathbf{F}_{ext}$. Therefore, the dynamic relation in (4) becomes

$$\boldsymbol{\Omega}(\mathbf{x})\ddot{\tilde{\mathbf{x}}} + (\mathbf{D_d} + \boldsymbol{\mu}(\mathbf{x},\dot{\mathbf{x}}))\dot{\tilde{\mathbf{x}}} + \mathbf{K}_d\tilde{\mathbf{x}} = \mathbf{F}_{ext}. \tag{6}$$

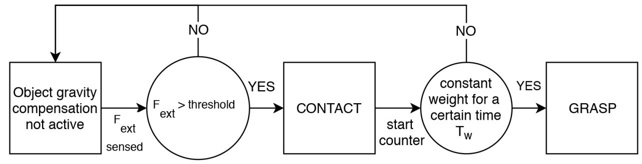

Fig. 1: Load compensation logic.

B. Load adaptation

When an object is grasped, the teleoperated robot must recognize it and autonomously compensate its weight. By doing that, the task of the object carrying is delegated to the gravity compensation term instead of the impedance controller. This will avoid any deviation from the reference trajectory due to the payload effect.

The external forces can be analyzed using the robot force/torque sensors to distinguish between the forces produced by temporal unexpected contacts (where there should be no compensation action), and by the weight of the grasped object (or a continuous external disturbance). In the latter case, an extra term that includes the payload on the end-effector should be added into the gravity/dynamics compensation part of the controller. We perform this by a state-machine logic (shown in Fig. 1):

- When the controller is initialized, the load compensation component term is disabled.
- If the sensed external force $\mathbf{F}_{ext}$ has a component greater than a certain threshold th_0 (in case of object grasping it is set along the negative z-axis direction), a timer counter starts and the object weight is calculated and saved (CONTACT state).
- If the sensed weight remains constant (or vary around a reasonably small range) for a certain period of time t_W, the algorithm assumes that the object has been grasped (GRASP state). Otherwise, the algorithm performs no compensation and returns to the initial state.

If the grasp condition is verified, the current external force vector is considered as the object's weight to be compensated

$$\mathbf{F}_{ob}(t) = -\mathbf{F}_{ext}(t). \tag{7}$$

To avoid a discontinuity in the time instant when the object weight is compensated, an exponential filter was implemented so that the actual compensation force is

$$\mathbf{F}_{comp}(t) = a_f\mathbf{F}_{ob}(t) + (1 - a_f)\mathbf{F}_{comp}(t), \tag{8}$$

where a_f is the smoothing factor.

When the load compensation term is active, the threshold must be updated by adding the current object weight $F_{ob,z}$, i.e., the z component of $\mathbf{F}_{ob}$, to the initial threshold value (th_0), so that the new threshold becomes $th_1 = th_0 + F_{ob,z}$. By doing this, unexpected external contacts are not considered as additional weights.

If the grasped object is suddenly lost, the impedance control term will generate fast and potentially dangerous robot movements that can be associated with the loss of passivity of the system. To avoid this, we developed a passivity-based contact stabilizer that is described hereafter.

C. Stability analysis in case of lost contact

To prove the stability of the system, we rely on a passivity-based control. We consider the whole system as a combination of subsystems, which can be described as input-output power ports $(\dot{\mathbf{q}}, -\boldsymbol{\tau})$ [11]. To prove that the overall system is passive, it is sufficient to prove that all the interconnected subsystems are passive.

Assuming that both the external environment and the master (i.e. the human operator) are passive, it must be proven that the controller on the slave side is passive with respect to the pair $(\dot{\mathbf{x}}, -\mathbf{F}_{ext})$. To study the energy balance of the system, it is convenient to use a storage function that can be defined as a positive semi-definite Lyapunov function $S : \mathbb{R}^m \rightarrow \mathbb{R}_+$, which is in our case equal to

$$S = \frac{1}{2}\dot{\tilde{\mathbf{x}}}^T \boldsymbol{\Omega}(\mathbf{x})\dot{\tilde{\mathbf{x}}} + \frac{1}{2}\tilde{\mathbf{x}}^T \mathbf{K}_d \tilde{\mathbf{x}} + m_{ob} g h + \frac{1}{2}\dot{\mathbf{x}}^T m_{ob} \dot{\mathbf{x}}, \quad (9)$$

in which there are the contributions of potential and kinetic energies deriving from both the impedance control and the object weight compensation force. Parameters m_{ob}, h and g are the object mass, its height with respect to the ground, and the scalar representation of the gravity acceleration, respectively. In this case, Cartesian velocity includes only translational parts, therefore $\dot{\mathbf{x}} \in \mathbb{R}^3$. The time derivative of (9) is

$$\dot{S} = \dot{\tilde{\mathbf{x}}}^T \mathbf{K}_d \tilde{\mathbf{x}} + \frac{1}{2}\dot{\tilde{\mathbf{x}}}^T \dot{\boldsymbol{\Omega}}(\mathbf{x})\dot{\tilde{\mathbf{x}}} + \dot{\tilde{\mathbf{x}}}^T \boldsymbol{\Omega}(\mathbf{x})\ddot{\tilde{\mathbf{x}}} + F_{ob,z}\dot{h} + \dot{\mathbf{x}}^T m_{ob} \ddot{\mathbf{x}} \quad (10)$$

where the last term denotes the effect of the object inertia in the dynamics of the system, which produces a force at the end-effector equal to $m_{ob}\ddot{\mathbf{x}}$. When the robot is moving, this term produces a force that will be applied at the end-effector in addition to the previously considered external force $\mathbf{F}_{ext}$ in (6). Therefore, after the object is grasped the new external force vector can be considered as

$$\tilde{\mathbf{F}}_{ext} = m_{ob}\ddot{\mathbf{x}} + \mathbf{F}_{ext}. \quad (11)$$

Now, the passivity should be studied w.r.t. the pair $(\dot{\mathbf{x}}, -\tilde{\mathbf{F}}_{ext})$. By combining (10) and (11) we get

$$\dot{S} = \dot{\tilde{\mathbf{x}}}^T \mathbf{K}_d \tilde{\mathbf{x}} + \frac{1}{2}\dot{\tilde{\mathbf{x}}}^T \dot{\boldsymbol{\Omega}}(\mathbf{x})\dot{\tilde{\mathbf{x}}} + \dot{\tilde{\mathbf{x}}}^T(-\boldsymbol{\mu}(\mathbf{x},\dot{\mathbf{x}})\dot{\tilde{\mathbf{x}}} - \mathbf{D_d}\dot{\tilde{\mathbf{x}}} - \mathbf{K_d}\tilde{\mathbf{x}} + \tilde{\mathbf{F}}_{ext}) + F_{ob_z}\dot{h}. \quad (12)$$

Considering that

$$\frac{1}{2}\dot{\tilde{\mathbf{x}}}^T(\dot{\boldsymbol{\Omega}}(\mathbf{x}) - 2\boldsymbol{\mu}(\mathbf{x},\dot{\mathbf{x}}))\dot{\tilde{\mathbf{x}}} = 0, \quad (13)$$

we have

$$\dot{S} = \dot{\tilde{\mathbf{x}}}^T \tilde{\mathbf{F}}_{ext} - \dot{\tilde{\mathbf{x}}}^T \mathbf{D_d}\dot{\tilde{\mathbf{x}}} + F_{ob,z}\dot{h}, \quad (14)$$

where the last term shows a variation of energy deriving from the end-effector velocity in the vertical axis direction, and $F_{ob,z} = m_{ob} g$. While the term $\dot{\tilde{\mathbf{x}}}^T \mathbf{D_d}\dot{\tilde{\mathbf{x}}}$ is positive, the sign of $F_{ob,z}\dot{h}$ is not known, thus the passivity condition $\dot{S} \leq \dot{\tilde{\mathbf{x}}}^T \tilde{\mathbf{F}}_{ext}$ can be potentially violated.

D. Energy tank

To solve the passivity condition issue, an energy tank based passivity controller can be added to the main control scheme. As explained in [13], the energy tank can be seen as a virtual reservoir filled with the energy dissipated by the system. This can be used as a *passivity margin* to implement non-passive actions. The dissipated power, expressed in (12) by the term $\dot{\tilde{\mathbf{x}}}^T \mathbf{D_d}\dot{\tilde{\mathbf{x}}}$, is used to store energy in the tank, whose state (denoted by x_t) is defined by

$$\dot{x_t} = \frac{\beta}{x_t}(\dot{\tilde{\mathbf{x}}}^T \mathbf{D}_d \dot{\tilde{\mathbf{x}}}) + u_t, \quad (15)$$

where β is a parameter used to stop the energy flow directed to the tank when a certain upper limit ϵ^u is reached. An excessive energy availability could lead to locally unstable actions, even if the system results as globally passive; hence, following [11], we define

$$\beta = \begin{cases} 1 & \text{if } T \leq \epsilon^u \\ 0 & \text{else} \end{cases} \quad (16)$$

with T being the tank level. The term u_t allows us to control the energy exchange from the tank to the main controller, and is set as $u_t = -\omega^T \dot{x}$, where $\omega(\mathbf{F}_{ext}, t)$ is the control input defined as

$$\omega(\mathbf{F}_{ext}, t) = \frac{\alpha}{x_t}(\mathbf{F}_{err}), \quad (17)$$

where $\mathbf{F}_{err}$ is the force error between the sensed external force $\tilde{\mathbf{F}}_{ext}$ and the force of object weight $\mathbf{F}_{ob}$ compensated by the controller, and can be formulated as

$$\mathbf{F}_{err} = \tilde{\mathbf{F}}_{ext} + \mathbf{F}_{ob}. \quad (18)$$

Considering that the load compensator is continuously compensating the object weight $\mathbf{F}_{ob}$, besides the passivity control action, this also provides a more robust classification between accidental disturbances and unsafe contact loss, which consequently result in a more compliant behaviour.

Parameter α is defined as

$$\alpha = \begin{cases} 1 & \text{if } T \geq \epsilon^l \\ 0 & \text{else} \end{cases} \quad (19)$$

and is used to stop the energy flow from the tank when its lower limit ϵ^l is reached.

The resulting total energy stored in the tank is

$$T(x_t) = \frac{1}{2}x_t^2, \quad (20)$$

where x_t must be strictly greater than zero, in order to avoid singularities [11], [13]. Next we apply the passivity control and the storage function is rewritten as

$$S_* = \frac{1}{2}\dot{\tilde{\mathbf{x}}}^T \boldsymbol{\Omega}(\mathbf{x})\dot{\tilde{\mathbf{x}}} + \frac{1}{2}\tilde{\mathbf{x}}^T \mathbf{K}_d \tilde{\mathbf{x}} + \frac{1}{2}x_t^2. \quad (21)$$

By following the same procedure as in (12), the time derivative of this new storage function can be derived as

$$\begin{aligned} \dot{S}_* &= \dot{\tilde{\mathbf{x}}}^T \tilde{\mathbf{F}}_{\mathbf{ext}} - \dot{\tilde{\mathbf{x}}}^T \mathbf{D_d}\dot{\tilde{\mathbf{x}}} + \dot{\tilde{\mathbf{x}}}^T \omega x_t + \beta(\dot{\tilde{\mathbf{x}}}^T \mathbf{D_d}\dot{\tilde{\mathbf{x}}}) - x_t \omega^T \dot{\tilde{\mathbf{x}}} \\ &= \dot{\tilde{\mathbf{x}}}^T \tilde{\mathbf{F}}_{\mathbf{ext}} - \dot{\tilde{\mathbf{x}}}^T \mathbf{D_d}\dot{\tilde{\mathbf{x}}} + \beta(\dot{\tilde{\mathbf{x}}}^T \mathbf{D_d}\dot{\tilde{\mathbf{x}}}). \end{aligned} \quad (22)$$

Due to (16), we have that

$$-\dot{\tilde{\mathbf{x}}}^T \mathbf{D_d} \dot{\tilde{\mathbf{x}}} + \beta(\dot{\tilde{\mathbf{x}}}^T \mathbf{D_d} \dot{\tilde{\mathbf{x}}}) \leq 0$$

therefore,

$$\dot{S}_* \leq \dot{\tilde{\mathbf{x}}}^T \tilde{\mathbf{F}}_{ext}, \tag{23}$$

which leads to the passivity condition. By including the passivity control action, the overall torque commanded to the robot joints is equal to

$$\boldsymbol{\tau}_c = \mathbf{J}(\mathbf{q})^T (\boldsymbol{F}_i + \alpha \mathbf{F}_{comp}), \tag{24}$$

with $\mathbf{F}_i$ being the impedance control action.

E. Contact recognition

For the studied interaction scenario, it is critical to distinguish correctly between cases of accidental contacts with external environment and cases when the carried object is lost. If these different types of contacts are correctly classified, the load compensation term can be activated only when it is necessary. To maintain a compliant behaviour, it is important that when an unknown contact occurs, only the low-stiffness impedance control should react to these interactions. To this end, we considered the force error in (17) as the unloading term instead of the total external force in the energy-tank control. However, this is not enough to completely avoid the tank discharge when "safe interactions" occur and may lead to an unsafe switching behaviour.

To overcome this issue we assumed that the previously referred safe interactions are characterized by a low velocity, while a sudden object-loss is characterized by a high velocity. With this hypothesis, we implemented an additional filtering action. If the contact velocity is below a certain threshold v_u, its contribution to the force error $\mathbf{F}_{err}$ is reduced. The new force error is therefore defined as

$$\tilde{\mathbf{F}}_{\mathbf{err}} = \begin{cases} \mathbf{F}_{err} & \text{if } \dot{\tilde{\mathbf{x}}} \geq v_u \\ C\mathbf{F}_{err} & \text{else} \end{cases} \tag{25}$$

where coefficient $C \in \mathbb{R}$ linearly varies from 0 to 1.

III. Experiments

The software architecture of the robot relies on XBot-Core [16] that was recently developed as open-source[1] and light-weight Real-Time (RT) platform for robotics. It was designed to be both an RT robot control framework and a software middleware, thus allowing code-portability between different robotic platforms. This software also provides a set of open-source plugins for the Gazebo simulator[2], which was used in the preliminary stages for code testing. We used the above-mentioned software to control a Kuka LWR arm in all experiments that we performed.

The energy-tank passivity controller was tested in situations before and after a contact loss by three experiments. In the first two experiments the contact loss happened when the robot was executing tasks autonomously, while in the last experiment we used a complete teleoperation framework for a grasping and manipulation task. In all experiments, the Cartesian stiffness values in transnational directions were set to constant low values, and the damping was set as a diagonal matrix with elements equal to $d_i = 2\xi_i\sqrt{k_i}$, where k_i are the diagonal elements of the stiffness matrix, and ξ_i is the damping coefficient set to 0.7.

To prove the validity of the peroposed contact recognition filtering action (as described in section II-E), a first set of experiments was designed by placing constant weights at the end-effector of a compliant robot (translational endpoint stiffness $\leq 300\frac{N}{m}$). When the weights were held in the air and compensated by the robot, we first induced external disturbances by manually pushing the end-effector along the vertical axis in both positive and negative directions. Finally, we suddenly dropped the grasped object from the end-effector, thus simulating an object-loss scenario.

The tank was initialized at its maximum level to study the maximum possible error due to the immediate object loss. This upper threshold was set to a low value in order to avoid an excessive energy storage from permitting unsafe motions (as explained in section II-C). The passivity controller was initialized when the load compensation actiaon started (GRASP state in Fig. 1) and was deactivated after it reached its lower limit. This was done to prevent the load compensation term from being switched on and off repeatedly during the object grasping (in which some error is expected during the transition phase of $t_W = 2s$), and to give a security margin after its deactivation.

The results of a typical experiment with the stiffness value equal to $200\frac{N}{m}$ and the applied object weight equal to $4Kg$ are illustrated in Fig. 2. Fig. 2a shows the load compensation force w.r.t. the total force. It is evident that the applied object weight was recognized and compensated correctly, and that the passivity controller was able to successfuly distinguish the other external disturbances coming from the environment (in this case the human arm was physically disturbing the

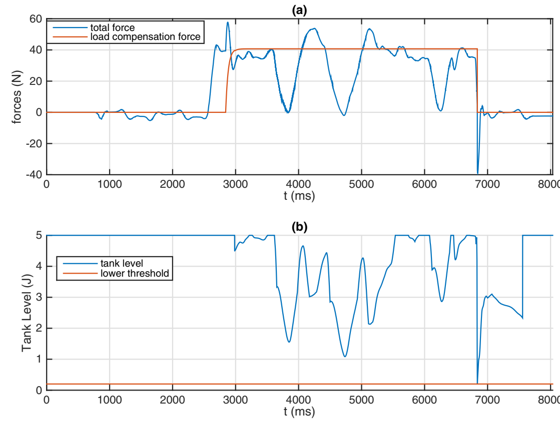

Fig. 2: Results with stiffness and applied load respectively equal to $200\frac{N}{m}$ and $4Kg$. Upper plots (a) show the load compensation force with relation to total force, while the lower plots (b) the tank level and the lower limit are illustrated. After that the tank reaches its lower limit, it remains detached from the rest of the controller until the load compensation is re-activated. This is done to avoid a switching behaviour.

[1]https://github.com/ADVRHumanoids/XBotCore
[2]https://github.com/ADVRHumanoids/GazeboXBotPlugin

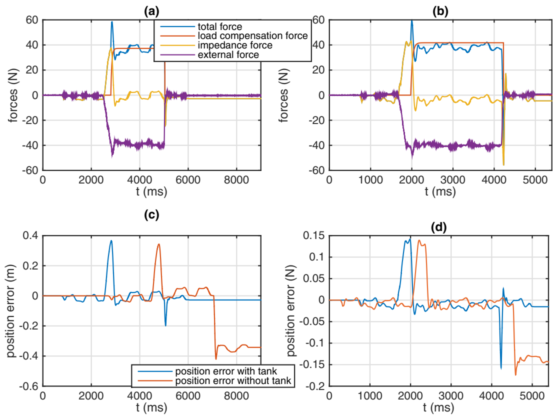

Fig. 3: Forces measured in the end-effector when applying a 4 Kg load with stiffness $K_d = 100\frac{N}{m}$ in (a) and $K_d = 300\frac{N}{m}$ in (b). The correspondent position errors are shown in (c) and (d) (blue curve). The orange curves in (c) and (d) represent the position errors obtained in the same experiments without the tank contribution.

robot) from the weight of the grasped object. Thus, there is no variation in the object weight compensation action during the period of time in which the load compensation is active. In that interval the tank level oscillation was as a result of the combined actions of its loading and unloading terms (expressed by (15) and (17) by the terms $\dot{\mathbf{x}}^T\mathbf{D}_d\dot{\mathbf{x}}$ and $\dot{\mathbf{x}}\tilde{\mathbf{F}}_{err}$). After the contact loss, we can observe an external force in the positive vertical direction. Since there was a high velocity, the contribution of $\mathbf{F}_{err}$ was not reduced and the tank level immediately reached its lower limit[3].

A. *Passivity controller performance evaluation*

The robot passivity controller was tested while the end-effector was moving along an eight-shaped trajectory in the $x - y$ plane. Position references were defined in the robot base frame as

$$\begin{aligned} x &= A\sin(2t) \\ y &= 2A\sin(t) \end{aligned} \tag{26}$$

where A is the amplitude and t the time of the sinusoidal trajectory. We conducted three trials, commanding translational stiffness references equal to $K_d = 100, 200$ and $300\frac{N}{m}$. For each trial, we placed weights of 3 and 4 Kg at the end-effector in two separate sub-trials. In the stiffest case ($300\frac{N}{m}$), the 3 Kg weight was not enough to show the effect of our passivity controller and was replaced by a 5 Kg weight. This was due to the fact that the higher stiffness value allowed the impedance controller to maintain a lower error and return the actual position to the reference position before the tank reached its lower limit.

The evaluation was performed before and after an unexpected loss of the manipulated object. Figure 3 illustrates the results of the experiments with a 4 Kg payload, with $K_d = 100\frac{N}{m}$ in (a) and (c), and $300\frac{N}{m}$ in (b) and (d). When the grasped object was detected, its weight was computed as explained in Fig. 1. Since its weight remained constant after a transition phase $t_W = 2s$, the estimated force was included into the load compensation term. Consequently, the deviations from the reference trajectory were reduced to zero. After that, the total force oscillated around the compensated load force as a result of the object inertia when the robot was moving. These effects were continuously corrected by the impedance control action.

When the contact was lost and when our method was not active, the load compensation term remained active, and the impedance controller settled around the opposite value of the object weight ($-30N$ or $-40N$). Due to the low value of the commanded stiffness, the impedance control action was not strong enough to return to the desired position reference. Because of that, the errors remained constant. On the other hand, when our method was active, the load compensation term was immediately detached (figures 3a and 3b); thus the impedance controller was able to return to its set-point, compensating for the errors. The different behavior with and without the energy-tank is evident by looking at the respective position error signals, showed in Fig. 3c and 3d. In both cases, when the tank was off, the position error after the contact loss was constant. On the other hand, when it was active, the sudden reaction of the controller keeps the error to a much smaller value in all trials.

Another important information given to us by the position error signal is that, when $K_d = 100\frac{N}{m}$ (Fig. 3c) the tank action reduced it by approximately 50%, and while when $K_d = 300\frac{N}{m}$, the difference was not very significant. Therefore our passivity controller gave its best contribution when low stiffness was commanded to the robot. By increasing the weight to 5 Kg, with the same stiffness, the difference became again more relevant. This happened because the error reduction is proportional to the applied load.

B. *Teleoperation*

In the last experiments, the human operator teleoperated a compliant robotic arm by providing Cartesian position references. To do so, we attached a set of optical markers to the operator's wrist. Marker positions were measured by an Optitrack system (Natural Point, Inc.) and were continuously sent to the Kuka robot controller via UDP. The robot was equipped with the Pisa-IIT SoftHand to allow the operator to perform the object grasping action. For these experiments, the Cartesian stiffness in all translational directions was set to a relatively low value ($K_d = 200\frac{N}{m}$).

Figure 4 shows the different phases of the teleoperation task. Starting from an initial configuration (Fig. 4a) the operator controlled the position of the robot arm in order to reach and grasp a 4 Kg object from the table (Fig. 4b). When the sensed external forces in the vertical direction exceeded the threshold, a similar procedure as described in section II-C was executed. In this case we used a transition phase $t_W = 6s$ to give enough time to the controller to preform an accurate measurement of the object weight that had to be compensated.

[3]The "bouncing" effect that could immediately reactivate it and cause potentially unsafe motion is seen in the tank level variation in Fig. 2b after the load compensation term in Fig. 2a is turned off. Nevertheless, the controller did not react to it thanks to the solution proposed in (25).

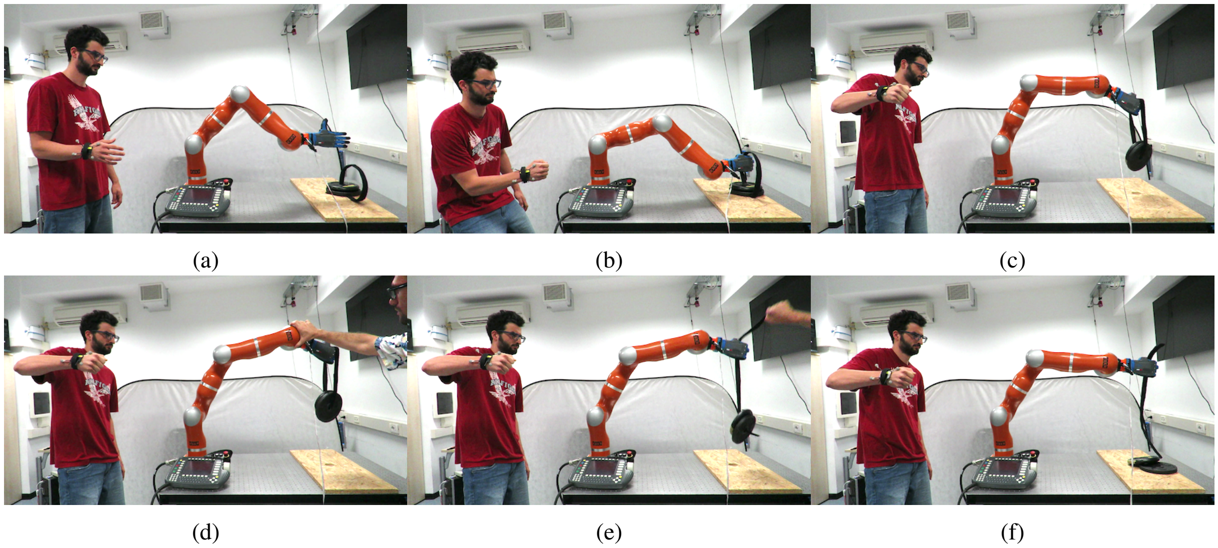

Fig. 4: Still frames of the teleoperation experiments with passivity controller.

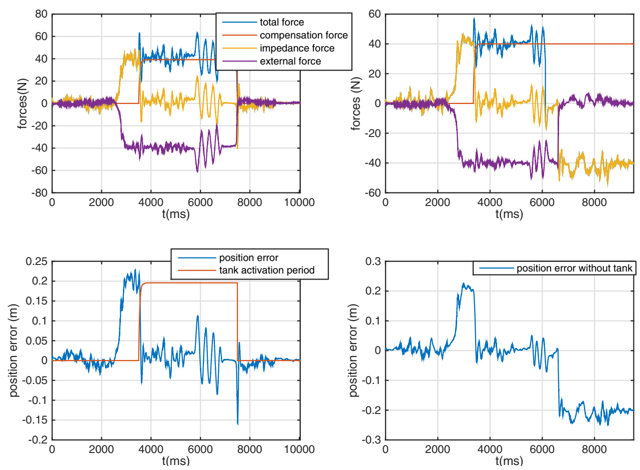

Fig. 5: Force and position measurements with (a and c) and without (b and d) the tank; the orange curve in c represents the time interval in which the tank is active.

During this period of time, the robot was not able to follow the operator's references due to the chosen low stiffness. When the sensed force remained constant after the 6 seconds period[4], the slave controller included it into the load compensated term (Fig. 4c) and the actual robot position returned to the reference position. Consequently, the robot was able to accurately follow the operator's movements while safely reacting to the external disturbances induced by another human (Fig. 4d). The tank did not completely unload and the load compensation term remained active, which demonstrates the controller's ability to distinguish different types of contact.

When an unexpected object-loss occurred (Fig. 4e) the tank unloaded and turned off the load compensation term. Therefore, the vertical position error was comparable to the results in the autonomous task. Consequently, the robot safely returned to the reference position with only the impedance control term active (Fig. 4f).

The same experimental procedure was also done without the proposed method. Figure 5 compares forces and position errors when the proposed method was used (left column) and when the proposed method was not used (right column). These comparison results are similar to the comparison results in the autonomous control trials in terms of spatial and temporal differences in position and force profiles, confirming that our approach is also successful in more complex tasks involving teleoperation.

IV. Conclusions and Future Work

The proposed semi-autonomous control action allowed the teleoperated robot to interact with an unknown external environment in a safe and compliant way. Moreover, the proposed passivity-based controller successfully distinguished between various types of contacts and therefore reacted differently when a sudden loss of a manipulated tool occurred (where an immediate detachment of the load compensation term was required), and when an external human perturbation was induced (in which case the robot was required to maintain a compliant behavior).

Although these preliminary results are satisfactory, the achieved performance might still be insufficient for applications that require extremely high precision tracking. A future improvement could focus on a more complex activation and deactivation actions of the load compensator, as a function of variations in the tank dynamics. A quicker object-weight estimation technique could also be implemented, to avoid huge position error that occurs in the beginning of the load compensating action, which is caused by the measurement time delay.

The most important improvement, however, could be the integration of the proposed method with the teleimpedance framework [4], [5], which enables the operator to command a variable stiffness to the robot in RT. To do so, an additional non-passivity term that arises from varying stiffness would have added to our controller (similar to [13]).

[4]Note that this time window can be adjusted.

References

[1] N. Diolaiti, C. Melchiorri, and S. Stramigioli, "Contact impedance estimation for robotic systems," *IEEE Transactions on Robotics*, vol. 21, no. 5, pp. 925–935, 2005.

[2] N. Hogan, "Impedance control - An approach to manipulation. I - Theory. II - Implementation. III - Applications," *ASME Transactions Journal of Dynamic Systems and Measurement Control B*, vol. 107, pp. 1–24, Mar. 1985.

[3] J. Heinzmann and A. Zelinsky, "Quantitative safety guarantees for physical human-robot interaction," *The International Journal of Robotics Research*, vol. 22, no. 7-8, pp. 479–504, 2003.

[4] A. Ajoudani, N. Tsagarakis, and A. Bicchi, "Tele-impedance: Teleoperation with impedance regulation using a body–machine interface," *The International Journal of Robotics Research*, vol. 31, no. 13, pp. 1642–1656, 2012.

[5] L. Peternel, T. Petrič, and J. Babič, "Robotic assembly solution by human-in-the-loop teaching method based on real-time stiffness modulation," *Autonomous Robots*, vol. 42, no. 1, pp. 1–17, Jan 2018.

[6] S. Chitta, E. G. Jones, M. Ciocarlie, and K. Hsiao, "Perception, planning, and execution for mobile manipulation in unstructured environments," *IEEE Robotics and Automation Magazine, Special Issue on Mobile Manipulation*, vol. 19, no. 2, pp. 58–71, 2012.

[7] G. Tonietti, R. Schiavi, and A. Bicchi, "Design and control of a variable stiffness actuator for safe and fast physical human/robot interaction," in *Robotics and Automation, 2005. ICRA 2005. Proceedings of the 2005 IEEE International Conference on*. IEEE, 2005, pp. 526–531.

[8] P. Landsmann, D. Paulus, and R. Kennel, "Online identification of load angle compensation for anisotropy based sensorless control," in *Sensorless Control for Electrical Drives (SLED), 2011 Symposium on*. IEEE, 2011, pp. 80–84.

[9] W. Kraus, V. Schmidt, P. Rajendra, and A. Pott, "Load identification and compensation for a cable-driven parallel robot," in *Robotics and Automation (ICRA), 2013 IEEE International Conference on*. IEEE, 2013, pp. 2485–2490.

[10] A. D. Luca and S. Panzieri, "Learning gravity compensation in robots: Rigid arms, elastic joints, flexible links," *International journal of adaptive control and signal processing*, vol. 7, no. 5, pp. 417–433, 1993.

[11] C. Schindlbeck and S. Haddadin, "Unified passivity-based cartesian force/impedance control for rigid and flexible joint robots via task-energy tanks," in *Robotics and Automation (ICRA), 2015 IEEE International Conference on*. IEEE, 2015, pp. 440–447.

[12] S. Stramigioli, R. Mahony, and P. Corke, "A novel approach to haptic tele-operation of aerial robot vehicles," in *Robotics and Automation (ICRA), 2010 IEEE International Conference on*. IEEE, 2010, pp. 5302–5308.

[13] F. Ferraguti, C. Secchi, and C. Fantuzzi, "A tank-based approach to impedance control with variable stiffness," in *Robotics and Automation (ICRA), 2013 IEEE International Conference on*. IEEE, 2013, pp. 4948–4953.

[14] A. Ajoudani, S. B. Godfrey, M. Bianchi, M. G. Catalano, G. Grioli, N. Tsagarakis, and A. Bicchi, "Exploring teleimpedance and tactile feedback for intuitive control of the pisa/iit softhand," *IEEE transactions on haptics*, vol. 7, no. 2, pp. 203–215, 2014.

[15] C. Ott, "Cartesian impedance control: The rigid body case," in *Cartesian Impedance Control of Redundant and Flexible-Joint Robots*. Springer, 2008, pp. 29–44.

[16] L. Muratore, A. Laurenzi, E. M. Hoffman, A. Rocchi, D. G. Caldwell, and N. G. Tsagarakis, "Xbotcore: A real-time cross-robot software platform," in *Robotic Computing (IRC), IEEE International Conference on*. IEEE, 2017, pp. 77–80.